

Title	Photonics of fullerene-conducting polymer composites and multilayered structures: new results and prospects
Author(s)	Yoshino, Katsumi; Yoshimoto, Kenji; Tada, Kazuya et al.
Citation	Proceedings of SPIE - The International Society for Optical Engineering. 2530 p.60-p.75
Issue Date	1995-12-08
oaire:version	VoR
URL	<a href="https://hdl.handle.net/11094/76959">https://hdl.handle.net/11094/76959</a>
rights	
Note	

***Osaka University Knowledge Archive : OUKA***

<https://ir.library.osaka-u.ac.jp/>

Osaka University

# PHOTONICS OF FULLERENE-CONDUCTING POLYMER COMPOSITES AND MULTILAYERED STRUCTURES: NEW RESULTS AND PROSPECTS

Katsumi YOSHINO, Kenji YOSHIMOTO, Kazuya TADA, Hisashi ARAKI, Tsuyoshi KAWAI,  
Masanori OZAKI and Anvar A. ZAKHIDOV\*

Department of Electronic Engineering, Osaka University, 2-1 Yamada-Oka, Suita, Osaka 565, Japan

\*On leave from Department of Thermophysics, Uzbek Academy of Science, Katartal 28, Tashkent 700135, Uzbekistan

## Abstract

The general features of charge transfer processes in fullerene / conducting polymer (CP) systems, such as energetics of photoinduced charge transfer (PCT) between  $C_{60}$  and CP  $\pi$ -electronic states, geometry of  $\pi$ - $\pi$  overlapping and the role of self-trapping effects to polaronic states on  $C_{60}$  and CP chains on the PCT dynamics are analyzed.

Persistent photoconductivity and electroluminescence quenching recently found in  $C_{60}$ /CP composites additionally to photoconductivity enhancement and photoluminescence quenching observed earlier, indicate that photogenerated  $C_{60}^{\cdot-}$  radicals may be extremely long living in CP matrices, due to multicharging of  $C_{60}$  as suggested by us accompanied with deep self-trapping to polaron/bipolaron states. The anisotropy of PCT is proposed to arise due to orientational modulation of overlapping between polaronic rings on  $C_{60}$  and CP which strongly suppresses back recombination. The strategy to increase the efficiency of  $C_{60}$ /CP donor-acceptor (DA) photocells by improving PCT is analyzed, particularly considering multilayered structures with polarization barriers at interfaces, and increased intralayer mobilities of carriers. To increase the efficiency of photons collection in photocells we suggest three layered D-M-A structures, with molecular "photon pump" layers strongly absorbing photons. The prospects for novel photonic applications of various  $C_{60}$ /CP systems, such as NLO devices and photomodulated field effect transistors (FETs) are discussed and illustrated by newest results. New results on superconductivity of  $C_{60}$ /CP upon alkali metal doping are presented, and exciting possibilities for novel superconducting phases in this system are discussed.

## 1. INTRODUCTION

We have proposed recently that fullerenes,  $C_{60}$  and  $C_{70}$ , can be used as weak acceptor dopants in conducting polymers (CP) and in a series of experiments have found quenching of photoluminescence (PL)<sup>1,2</sup> and the enhancement of photoconductivity (PC)<sup>2,3</sup> due to photoinduced CT between fullerene and a number of CP<sup>4-7</sup> as earlier suggested<sup>8</sup>. Photoinduced CT (PCT) from  $C_{60}$  to CP has been independently found also in other CP, like MEH-PPV and proved by other complementary methods, like photoinduced absorption (PA), light induced ESR<sup>10</sup> and recently studied by transient time spectroscopy, clarifying rather fast time of forward PCT process<sup>11</sup>.

It has been found also that sizable PCT at the interface between  $C_{60}$  films with various CP leads to photovoltaic effect, which opens interesting perspectives for solar cell applications<sup>10,13</sup>. We showed also that electroluminescence is quenched even much more stronger indicating that  $C_{60}$  molecule acts as a multiple trapping and/or recombination center for carriers. On the other hand PC in non-degenerated ground state CP and also in CP with degenerated ground state such as polyacetylene derivatives is enhanced significantly upon fullerene doping at the excitation in three spectral regions: the wavelengths of (a) the interband transition in CP ( $h\nu > 2\Delta$ ,  $2\Delta$  being a gap in CP) and (b) allowed ( $h\nu \rightarrow t_{1g}$ ) and (c) forbidden ( $h\nu \rightarrow t_{1u}$ ) optical transitions in fullerene.

Remarkable polarity effect was observed in the spectral response of enhanced PC, proving that positively charged mobile carriers (polarons  $P^+$ ) in polymeric chains contribute to PC.

The effect of persistent photoconductivity (PPC) has been found in  $C_{60}$ /CP nanocomposites and we have studied on its dependence on  $C_{60}$  concentration, light intensity and temperature. We discussed the general scenario of photophysical processes in  $C_{60}$ /CP systems and show that photoinduced CT can take place in two qualitatively different channels: either upon photoexcitation of CP or due to absorption in  $C_{60}$ .

Observations of PPC and enhanced quenching of EL in  $C_{60}$ /CP systems<sup>7</sup> suggest that  $C_{60}$  is rather unusual type of weak dopant which shows more interesting physical behavior compared to other photosensitizing weak dopants like oxygen or dyes. It was pointed that for the strong time anisotropy of PCT, i.e. ultra fast forward PCT from CP to  $C_{60}$  and strongly delayed backward CT recombination from  $C_{60}$  to CP, the self-trapping to string type polarons on  $C_{60}$  spheres is important for the charge transfer processes between  $C_{60}$  and CP due to 1) orientational modulation of  $\pi$ - $\pi$  overlapping between  $C_{60}$  and CP and 2) gain in renormalization energy.

In the present work we discuss the energetics and dynamics of PCT and emphasize following new topics:

1. Discuss the efficiency of CP/C<sub>60</sub> heterojunctions based solar cells, in the concept of Donor-Acceptor molecular photocell, which is further developed and the ways to enhance their efficiency are analyzed. Particularly the enhanced carriers separation by polarization barriers and increased collection of photons by "photon pump" dye layers in multilayered structures are suggested.
2. Demonstrate that Schottky-type diodes are found at CP/C<sub>60</sub> composites-metal contact and show enhanced photovoltaic response with C<sub>60</sub> concentration. We discuss the role of C<sub>60</sub> in the enhancement of their photoresponse.

In all the above studies charge carriers appeared in CP/C<sub>60</sub> composites only due to intrinsic CT between C<sub>60</sub> and CP upon photopumping, and it is interesting to study the effects of extrinsic CT in the ground state provided by n- or p-type doping of such composites, when charge carriers can be transferred from external (to CP/C<sub>60</sub> system) second intercalant (K or I<sub>2</sub>) both to CP chains and C<sub>60</sub> molecules. Optical and conductive properties of such system are very intriguing, while at low temperatures the appearance of superconductivity (SC) has been proved by us<sup>14</sup>.

C<sub>60</sub> are known to be aggregated into clusters in CP/C<sub>60</sub> composites (at least at large C<sub>60</sub> content<sup>15</sup>), then doping creates K<sub>3</sub>C<sub>60</sub> granules, which being connected by proximity effect through conducting CP, or by Josephson junctions through insulating CP barriers, giving an interesting example of disordered granular SC. We here discuss some of their properties studied by low field microwave absorption (LFMA) and SQUID magnetometry. At small C<sub>60</sub> concentration, when C<sub>60</sub> is in monomolecular phase we expect appearance of novel SC phase in which pairing of electrons in CP chains can be induced by hybridization with intercalated C<sub>60</sub> molecules.

Superconductivity in poly(3-alkylthiophene)-C<sub>60</sub> composite (PAT-C<sub>60</sub>) is found upon doping by potassium from vapor phase. The superconducting transition at T<sub>c</sub>=17K is detected by SQUID magnetometry, which showed 0.1 % of superconducting fraction for 5 mol% C<sub>60</sub> content. Exceptionally strong LFMA implies the granular superconducting phase. Rather small hysteresis of LFMA indicates the important role of Josephson weak links network, probably formed between superconducting K<sub>3</sub>C<sub>60</sub> clusters separated by conductive K<sub>x</sub>PAT barriers. Electron spin resonance (ESR) of PAT(C<sub>60</sub>)<sub>x</sub>K<sub>1-x</sub> composite shows two types of lines: one from negative polarons P<sup>-</sup> in PAT chains, and other lines are assigned to K<sub>3</sub>C<sub>60</sub> clusters.

## 2. EXPERIMENTAL

Conducting polymers, poly(3-alkylthiophene) (PAT), poly(9,9-dialkylfluorene) (PDAF), poly-(2,5-dialkoxy-*p*-phenylenevinylene) (RO-PPV) and poly(*o*-trimethylsilylphenylacetylene) (PTMSiPA) were prepared and purified by the methods already reported<sup>16-19</sup>. All these polymers are soluble in conventional solvents such as toluene and chloroform. C<sub>60</sub> and C<sub>70</sub> prepared by an arc discharge utilizing graphite as an electrode and washed with toluene, was used in this experiment. C<sub>70</sub> prepared by same method was also used.

Both fullerene (C<sub>60</sub> and C<sub>70</sub>) and CP of appropriate molar ratio were dissolved in toluene, and thin films were prepared by casting the solution on an ITO (In-Sn Oxide) coated and noncoated quartz plates. Gold deposited by evaporation on the film served as a second electrode.

Layered structure of C<sub>60</sub>/CP was prepared by the vacuum deposition of layer C<sub>60</sub> onto a CP film which was formed on a gold evaporated layer over a quartz plate. Then the aluminum layer was deposited by evaporation on it as a second electrode.

Absorption and fluorescence spectra were measured by utilizing a spectrophotometer Hitachi 330 and fluorescence spectrophotometer Hitachi F-2000. Steady-state PC was measured by irradiating a Xe arc lamp light passing through a monochromator on the sample.

The free standing films of PAT-C<sub>60</sub> with various C<sub>60</sub> content, (0.5; 2.5; 5; 10 mol%) were placed into 5 mm diameter ESR quartz tubes, on the other end of which metallic K was inserted. The tubes were then heated in the double furnace. The derivation of microwave absorption measurements were carried out using a Varian E-112 and Bruker ESR-300 spectrometers operating at 9.1-9.6 GHz with the field modulation frequency of 100 kHz. DPPH was used as a marker of g-factor and a reference of ESR intensity. An Oxford Instruments ESR-900 cryostat allowed the temperature variation from 5K to 300 K with + 0.2 K precision. Additionally equipped external dc Helmholtz coils allowed the H-field scanning through zero from -50 to +50 G. (details of LFMA method were reported in Ref. 20.) Magnetization was measured in Quantum Design SQUID, model MPMS2.

## 3. EXPERIMENTAL RESULTS

### 3.1 Photoconductivity Enhancement and Photoluminescence Quenching

#### 3.1.1 NDGS conducting polymers

In CPs with non-degenerated ground state (NDGS CP) such as PAT, PDAF and RO-PPV, PL was quenched remark-

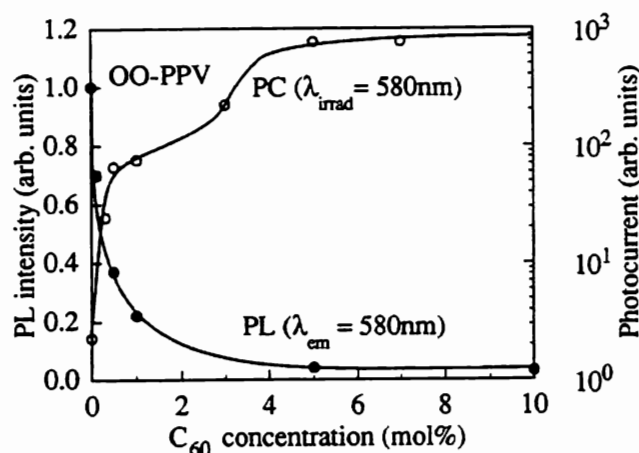


Fig.1 Dependence of PL intensity and photocurrent of  $C_{60}$ /OO-PPV composite film on the concentration of  $C_{60}$ .

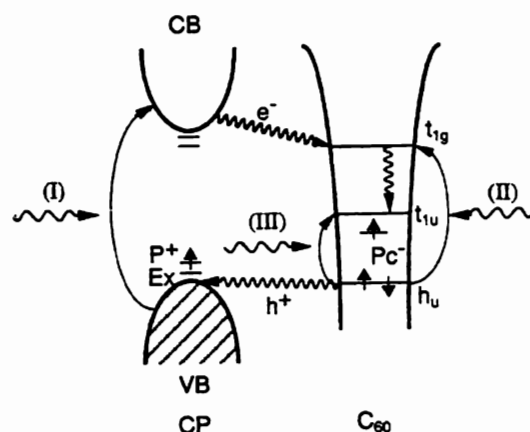


Fig.2 Energy diagram of OO-PPV and  $C_{60}$ .

ably and PC was enhanced intensively as evident in Fig.1 upon doping of small amount of  $C_{60}$ .

It should be mentioned that the PC was enhanced in the wavelength range corresponding to (I) the inter-band transition in CP, (II) allowed transition in  $C_{60}$  ( $h_u \rightarrow t_{1g}$ ) at 3.5 eV (peak) and also (III) the forbidden transition in  $C_{60}$  ( $h_u \rightarrow t_{1u}$ ) at 1.8 eV.

These results can be explained by the dissociation of exciton-polaron in CP upon collision with  $C_{60}$  and PCT between CP and  $C_{60}$  as schematically shown in Fig.2. The scenario of photogeneration for NDGS CP case will be discussed in the latter section.

### 3.1.2 DGS conducting polymer

Contrary to NDGS CP, quenching of PL by  $C_{60}$  doping can not be studied in PTMSiPA which has degenerated ground state (DGS) structure and shows no fluorescence even in the non-doped state. However, the PC was found to be enhanced upon  $C_{60}$  doping just as in the case of NDGS CP in the wavelength also corresponding to (I) the inter-band transition, (II) excitation due to allowed transition in  $C_{60}$  and (III) forbidden transition in  $C_{60}$ .

Figure 3 shows the photoconduction spectra of  $C_{60}$  doped PTMSiPA film. It should be mentioned that PC is remarkably enhanced upon  $C_{60}$  doping. In these spectra we can confirm a sharp peak at around 1.8 eV, wide peak at around 3.5 eV and also broad response in a wide band at 2.0-3.0 eV. If these responses are compared with the absorption spectrum a sharp peak can be attributed to the forbidden transition of  $h_u \rightarrow t_{1u}$  in  $C_{60}$ , a wide peak at 3.5 eV to the allowed transition of  $h_u \rightarrow t_{1g}$  in  $C_{60}$  and the broad structureless response at 2-3 eV to their inter-band excitation in PTMSiPA. It should also be noted that strong polarity effect exists in PC spectrum.

### 3.1.3 Scenario of Enhanced Photogeneration Processes

The enhancement of PC can be understood from the scenario of the photogeneration and photoexcited charge transfer processes.

#### NDGS CP Scenario

In the spectral range (I), photoexcited intrachain exciton-polaron (Ex-P) migrates along polymer main chain and when it encounters with  $C_{60}$ , electron may be favorably transferred to  $C_{60}$  and relaxes to negative polaron ( $Pc^-$ ) and enhancement of PC due to the migration of positive polarons ( $P^+$ ) on polymer main chain occurs. Note that in pure (undoped) NDGS CP only interchain separation of  $P^+$  from  $P^-$  can give PC, which is rather small due to weak interchain hopping. Presence of  $C_{60}$  molecules allows electron to be captured on it, separated spatially from  $P^+$  on the chains, which suppresses recombination and thus increases concentration of charge carriers. In the case of photoexcitation in the wavelength region (II) and (III), electron is excited from  $h_u$  to  $t_{1g}$  and  $t_{1u}$ , respectively in  $C_{60}$  and the hole in  $C_{60}$  should be transferred to the valence band of conducting polymer (where it relaxes to  $P^+$ ) which again contributes to enhancement of the PC.

#### DGS CP Scenario

When  $C_{60}$  molecules are doped between chains of PTMSiPA the following two new channels open for the enhancement of photogeneration.

**A.  $C_{60}$  Excitation channel:** By absorbing photon of around 3.5 eV, electron is excited from  $h_u$  to  $t_{1g}$  in  $C_{60}$ . The electron

in  $t_{1g}$  relax to  $t_{1u}$  and should stabilize as a polaron  $Pc^-$  in  $C_{60}$  due to strong interaction with phonons or in the other words due to formation of Jahn-Teller type distortion, while hole is transferred to polymeric chain. The transition from  $h_u$  to  $t_{1u}$  at 1.8 eV is a forbidden transition but, as we have proved for the case of  $C_{60}$  inside RO-PPV matrix still electron will be excited with some probability to  $t_{1u}$ , due to change of  $C_{60}$  symmetry in the polymeric environment. And then it also stabilizes to  $Pc^-$  on  $C_{60}$ , as soon as hole from  $h_u$  level will be transferred to valence band of PTMSiPA, which should be stabilized forming charged (positive) polaron  $P^+$ .  $P^+$  can not transfer directly to more energetically stable state of  $S^+$  soliton due to topological restrictions but upon collision with neutral  $S^0$  soliton, it will transform to charged  $S^+$ , which contributes to the PC. So here  $C_{60}$  plays a role of "photon pump", which injects holes into polymeric chains, creating additional  $S^+$ , and thus giving rise to PC enhancement.

**B. PTMSiPA Excitation Channel:** By the irradiation of light with photon energy exceeding 2.0 eV  $P^+-P^-$  pairs should be created at adjacent chains by interchain absorption or (at  $h\nu \gg 2\text{eV}$ ) in the same chain due to intrachain absorption in PTMSiPA and migrate along polymer main chain until meet  $C_{60}$  molecule. When the polaron  $P^+$  encounters with  $C_{60}$ , electron will be favorably transferred to  $C_{60}$  decreasing the probability to recombine with  $P^+$ , which on its turn will form  $S^+$  through collisions with  $S^0$  or another  $P^+$ . This  $S^+$  will contribute to enhanced PC since the recombination of  $S^+$  with  $Pc^-$  on  $C_{60}$ , (which is a belt-like deformation around  $C_{60}$  sphere) should be suppressed due to self trapping effects, which should decrease the overlapping between  $Pc^-$  and  $S^+$  wave functions due to deformational and some other geometrical reasons. We shall discuss this phenomena in detail elsewhere. So  $Pc^-$  states are long living ones as has been found recently by transient-time spectroscopy by Vardeny et al.

So  $C_{60}$  plays a role of sensitizer in both NDGS and DGS CPs.

### 3.1.4 Polarity Effect on Photoconductivity

As evident in Fig.3, in PTMSiPA remarkable polarity effect was observed in the enhanced PC spectrum. That is, only for the light irradiation from positive electrode side, large signal was observed in the wavelength regions (I) and (II). However in the range of (III), for both negative and positive polarities, that is, for excitations both from the cathode side and anode side similar magnitude of photoresponse was observed.

This is explained clearly by the migration of photogenerated positive carriers in CP, because in the ranges (I) and (II) the carrier can be only photogenerated at the area near the irradiated-side electrode. The fact that the PC was observed for the case of the positive polarity means that predominant migrating carriers are positive carriers, most probably charged solitons, migrating through the bulk of the sample to negative electrode. However in range (III) carrier is uniformly generated in the bulk of sample. Therefore polarity of the applied voltage has no effect in the later case.

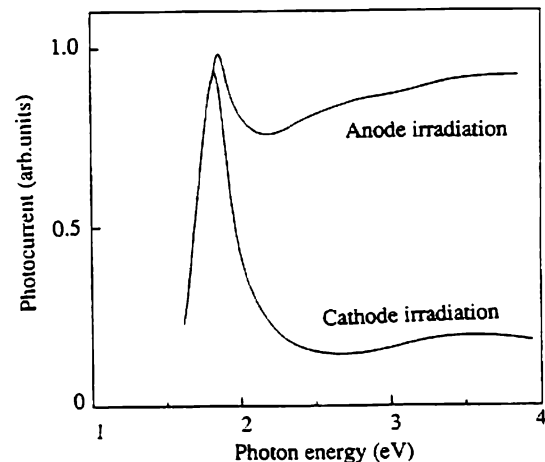


Fig.3 Photocurrent spectra of  $C_{60}$ /PTMSiPA composite film.

### 3.2 Persistent Photoconductivity

We have observed even at low pumping density the effect of PPC (i.e. the memory effect of dark conductivity enhancement due to residual charges after switching off the light source), depending on the spectral range used for photoexcitation. Annealing can restore the initial low dark conductivity, confirming that charges are accumulated in some deep traps, meaning that recombination of charges is strongly suppressed.

Typical photoconductive response in  $C_{60}$  doped PAT-18 upon irradiation of light pulses of 1.8 eV in photon energy is shown in Fig.4. Similar behavior was also observed upon excitation with photons of 2.2eV and 3.5eV. As evident in this figure, the photoresponse was found to be composed of two parts: a fast part and a slow part. That is, upon irradiation of a light pulse photoconduction increases in step wise then continues to grow slowly during the pulse width of light. Upon shutting off the light, the photocurrent decreases by some amount in step-wise and then the remaining part decreases very slowly. The decay time of remanent components extremely long compared with the prompt component. This remanent component of PC can be called as PPC. Therefore, the slowly increasing part of PC under the pulse light irradiation may

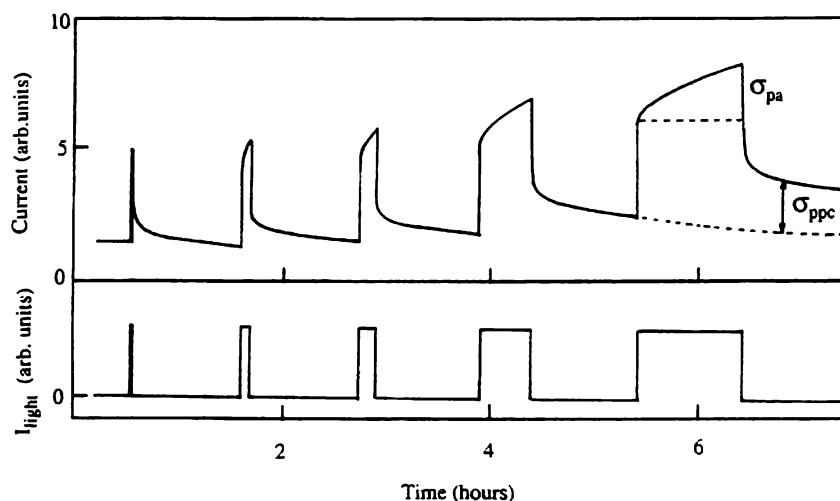


Fig.4 Typical photoconductive response in doped  $C_{60}$ /PAT-18 composite film upon irradiation of light pulses(1.8eV).

be originated in the accumulation of persistent photoconducting carriers. This interpretation is consistent with the pulse width dependence of photocurrent. That is, the slow rising component  $\sigma_{pa}$  increases as the pulse width increases and the persistent conductivity also increases, tending to saturate.

The existence of PPC means that the recombination probability of the separated positive (in PAT-18) and negative (in  $C_{60}$ ) charges is strongly limited. There seems to be several possibilities for the suppression of the recombinations;

- (1) Change of the charge distribution in  $C_{60}^-$  from the initially captured state, that is, rotation of charge belt results in the smaller overlapping interaction with main chain  $\pi$ -system.
- (2) The further stabilization of  $C_{60}^-$  to  $C_{60}^{2-}$  bipolaron  $BP_c^{2-}$ .
- (3) The disorder of the conformation of polymer main chain and resulting fluctuation of the electronic band scheme of CP with long side chain may also contribute for the suppression of the recombination of separated carriers.

The magnitude of PPC increases with increasing concentration of  $C_{60}$ . However at higher  $C_{60}$  doping level, it tends to saturate (or decrease again). Dependences of PPC on light intensity and also temperature were also studied. With increasing light intensity, PPC increases, tending to saturate. At higher temperature, the PPC in PAT-18 is found to tend to decrease. The recombination of  $P^+$  on polymer chains with the charge on  $C_{60}$  may be slowed down slightly by poor overlapping of  $BP_c^{2-}$  and possibly  $TP_c^{3-}$  with  $\pi$ -orbital of polymer. On the other hand their interaction with exciton (Ex) is possible. Some of above reactions are spin selective and hence can be influenced and checked by external magnetic field.

### 3.3 Photoluminescence Quenching and Electroluminescence Quenching

We have reported that in CPs with non-degenerated ground state (NDGS CP) such as PAT, PDAF and RO-PPV, PL was quenched notably upon  $C_{60}$  doping as shown in Fig. 1 for example in RO-PPV<sup>1,3</sup>, which can be explained by the dissociation of Ex or Ex-P on CP main chains upon collision with  $C_{60}$  and highly effective charge transfer.

However, we have found that electroluminescence (EL) is more intensively quenched than PL.

Recently, conducting polymers, PAT, PDAF, PPV and PPV-derivatives have been demonstrated to be used as an active light emitting layer in EL-diode by sandwiching with cathode and anode electrodes. We already reported that molecularly doped CP exhibits also unique characteristics as the light emitting layer in an EL diode. We have also studied effects of  $C_{60}$  doping on emission characteristics of EL diode based on CP.

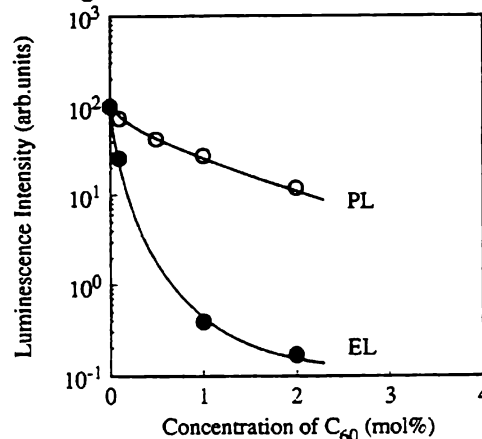


Fig.5 Dependence of the PL and EL intensities on the concentration of  $C_{60}$ .

EL is found to be quenched upon  $C_{60}$  doping as shown in Fig.5 for example in the EL diode of Mg-In/OO-PPV/ITO structure, though the emission spectrum does not show notable change. It should be noted in this figure that EL quenching by  $C_{60}$  is much more dramatic than PL quenching. The stronger EL quenching can be explained by taking the process of EL emission into consideration as follows.

In CP EL diode, electrons (or negative polarons  $P^-$ ) and holes (or positive polarons  $P^+$ ) are injected into CP from cathode and anode, respectively. Either one type or both types of carriers migrate crossing electrode distance under biased electric field. Upon encountering of electrons( $P^-$ ) to holes( $P^+$ ), excitons (actually self-trapped Ex-P, which we denote for simplicity as Ex) will be formed and the radiative decay of those excitons is the origin of the EL emission.

Therefore,  $C_{60}$  doped in CP may play a complicated role: (1) induce dissociation of Ex, and (2) capture carriers (either both  $P^-$  and  $P^+$  or one of them). The existence of the second process may be the origin of stronger quenching effect in EL than in PL.

It should be mentioned that the EL quenching effect did not depend strongly on the thickness. That is, the quenching ratio of EL intensity was just similar for different thickness of EL diodes.

The fact that EL quenching effect by  $C_{60}$  is not influenced by the thickness of CP suggests that only one type of carrier transits between electrodes and it is not trapped by  $C_{60}$  before encountering with opposite polarity of charge and forming of excitons. Therefore, excitons must be formed in the area near one of two electrodes, resulting in EL emission from this area. In most CP, majority photocarriers are positive carrier (holes or  $P^+$ ). Then it is reasonable to consider that holes ( $P^+$ ) transit from the anode to the cathode without severe trapping by  $C_{60}$  and forming excitons at the area near the cathode. This is consistent with electronic band schemes, according to which HOMO of  $C_{60}$  ( $h_u$ -level) is much lower than top of the valence band and electronic level of  $P^+$  in RO-PPV, making hole transfer to it unfavorable.

On the other hand, electrons (or  $P^-$ ) can be captured by  $C_{60}$ , because the conduction band bottom (LUMO) of RO-PPV is located at energy higher than the LUMO ( $t_{1u}$ ) of  $C_{60}$ . Therefore, the experimental results suggest that the injected electron ( $P^-$ ) from the cathode are effectively captured by  $C_{60}$  forming  $C_{60}^-$  (or actually the negative polaron of the belt type deformation around the perimeter of  $C_{60}$  sphere) during migration of short distance before encountering hole ( $P^+$ ), effectively resulting in the formation of smaller density of excitons at the area near the cathode. Even if Ex has a chance to be formed it should be also dissociated by the interaction with neutral  $C_{60}$  or its ions  $C_{60}^n$ . It is also probable that even polaron on  $C_{60}^-$  ( $P_c^-$ ) may capture second electron, since according to numerous theoretical predictions two electrons prefer to occupy the same  $C_{60}$  rather than two different molecules, forming dianion or bipolaron  $BP_c^{2-}$ ,  $C_{60}^{2-}$ , either due to effectively negative Hubbard  $U$  or/and due to stronger self-trapping effect. Due to very strong electron accepting ability, it is not excluded at the present stage that even third, forth and  $n$ -th electrons can be captured by the same  $C_{60}$  molecule forming  $C_{60}^{3-}$ ,  $C_{60}^{4-}$ ,  $C_{60}^{n-}$  respectively. These facts indicate that  $C_{60}$  may be very strong multiple trapping center for carriers, which to our knowledge was not observed for any other impurities.

It should be mentioned that  $C_{60}^{n-}$  formed by capturing negative carriers can then be extremely effective recombination center for holes ( $P^+$ ) due to unusually strong Coulomb attraction between them,  $n$ -times enhanced. By this non-radiative recombination,  $C_{60}^{n-}$  turns to  $C_{60}$  and becomes again effective trap for electrons. Very roughly speaking, if this picture is true, then  $C_{60}$  at concentration  $m\%$  acts effectively as at concentration of  $(nm)\%$ , due to its multiple trapping effect, i.e. effect of each  $C_{60}$  is  $n$ -times enhanced. This picture needs further investigation, since due to charging of  $C_{60}$  one should consider space charge limited current in EL diode in multiple charging limit.

Anyway the  $C_{60}$ /CP EL diode may serve as an ideal system to study the multiple charging effect on  $C_{60}$ , and especially to check the existence of  $BP_c^{2-}$  which are believed to play an important role in superconductivity of alkali-metal fullerenes by various modulation spectroscopy methods. This work is in progress currently.

## 4. DISCUSSION: Photoinduced CT between $C_{60}$ and CP

### 4.1. Energetics of PCT

Charge transfer between CP and the intercalated dopant is known to be governed by energetics, i.e by relative energies of occupied (HOMO) and empty (LUMO) electronic states, and by the overlapping of their orbitals. Depending on the energetics dopants can be viewed as strong or weak ones, as sketched at Fig.6 a) and b). Strong donors (e.g.  $n$ -type dopants like Na or K) have their HOMO above the bottom of conduction band in CP, while strong acceptors, ( $p$ -type, like  $I_2$  or  $AsF_6$ ) have their LUMO below top of valence band, i.e. both are outside the band gap  $2\Delta$  of CP, and the CT takes place in the ground state (GS). Contrary weak dopant : weak donors (D) ( or weak acceptors (A)) have their HOMO ( or LUMO ) levels lying within the energy gap of polymer ( as shown in Fig.6 ). In this case the charge can not be favorably transferred to polymeric chain in the GS, however upon photoexcitation electron may be transferred from  $D^*$  to conduction band ( or hole from  $A^*$  to valence band ) of chain forming polarons  $P^-$  in CP.

It is clear that photoexcitation of  $D \rightarrow D^*$  or  $A \rightarrow A^*$  may lead to creation of  $P$  in the chain even at  $h\nu < 2\Delta$  due to electron tunneling from  $D^*$  or  $A^*$  levels to states of polymeric chain and cause the enhancement of PC in the absorption band of  $D$  or  $A$  which play thus role of dyes for photosensitization of  $PC^8$ .

On the other hand  $Ex$  photocreated in chains may be quenched by  $D$  and  $A$  weak dopants either through energy transfer or by electronic transfer between  $D$  ( $A$ ) and  $Ex$  levels. So oxygen is a simplest case of such weak acceptor and it enhances PC e.g. of PAT and changes ESR of PPP due to CT processes<sup>8,9</sup>. The rate of CT processes: both forward PCT charging and backward recombination depends on the overlapping integral  $t$  between corresponding states.

Thus  $C_{60}$  is a weak dopant for most CP like PPV, while it can be nearly strong dopant for low energy gap CP.

Contrary to other molecular weak dopants fullerenes have the following advantages:

1.  $C_{60}$  has an extended system of two-dimensional (2-D)  $\pi$ -electrons, which should have strong overlapping with 1-D  $\pi$ -electrons of CP chains, with  $t \sim 0.1-0.3$  eV, which should make the forward CT processes between them an extremely quick one, as indeed observed<sup>10-12</sup>. Note that interaction of  $C_{60}$  with nonaromatic polymers, do not lead to enhanced PC<sup>22</sup> and PL quenching<sup>23</sup> thus supports the important role of  $\pi$  electrons for CT.
2. Due to 2-dimensionality of electronic states  $C_{60}$  spheres should pronounce self-trapping effect which lead to formation of P/BP and self trapped excitons of string type<sup>24,25</sup>. This string type trapped electrons should play important role in CT processes between P/BP and  $Ex$  of CP chains and may cause new features in their interactions.
3. Fullerenes have a large size, and hence the suppressed Coulomb repulsion of charges on the buckyball. Together with large electron affinity this may lead to multiple charging of  $C_{60}$  upon CT. Moreover due to large size,  $C_{60}$ , should deform chains and create defects; while the CP chains on their turn should deform  $C_{60}$  molecules, changing their symmetry (as we have proved by observation of forbidden optical transitions at 1.8 eV in  $C_{60}$  upon intercalation into CP<sup>5</sup>).

This features can influence the dynamics of the PCT process and we discuss below some new aspects of PCT in the context of newest experiments.

#### 4.2. Polarons/Bipolarons on $C_{60}$

It has been shown recently in simple SSH model that excitations on  $C_{60}$  should be self-trapped (ST) forming  $Pc$ ,  $BPc$ <sup>25,26</sup>, which is quite natural, since in 2-D system ST is always favorable and takes place without ST barrier. What was surprising is the geometry of ST states, which has a form of a string around the  $C_{60}$  sphere, as sketched at Fig.7. Later the ST problem has been addressed in approaches more sophisticated than SSH<sup>26</sup>, and it was shown that  $Pc^-$  has a uniform charge distribution, since the ST ring easily rotates by tunneling between equivalent minima, while doubly charged states ( $Exc$ ,  $BPc^{2-}$ ) are really of localized ring type. We stress here that this geometry of ST states may have an important effect on the CT process since overlapping of ST states with CP is now depending on the orientation of the ring relatively to the chain (shown schematically at Fig.7). This makes forward and back CT processes

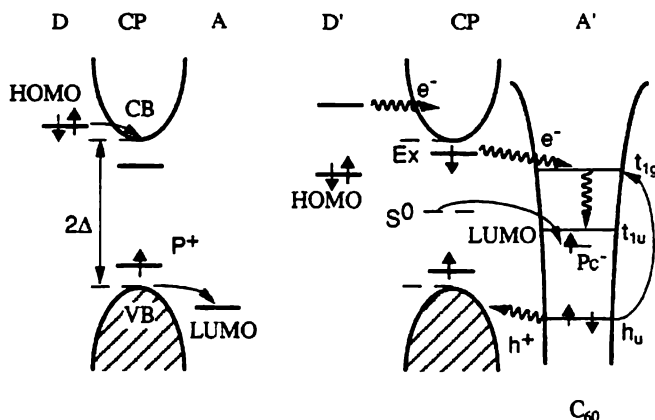


Fig.6 Energy diagram of Strong( $D,A$ ) dopant and Weak( $D',A'$ ) dopants in CP.

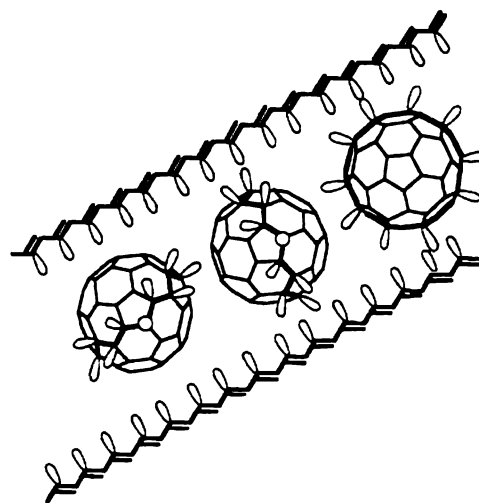


Fig.7 Geometry of overlapping between string BpC and PC.



nonequivalent, since forward CT goes to free  $\pi$ -states of  $C_{60}$ , (which are well overlapped with those of chains), it is fast  $t_{tr} = 1/t = 10^{-16}$  sec, while back CT from ST ring to CP may be suppressed, depending on the geometry of ST state and its orientation. If one assumes that  $P_c^+$  are uniform, while  $BP_c^{2-}$  are localized rings, then  $BP_c^{2-}$  should be long living states, since their recombination with  $P^+$  on chains is slower due to in average smaller overlapping of arbitrary oriented ring and chain. This might be one of the explanation for the PPC, which originates from accumulated long lived  $P^+$ , countercharges of  $BP_c^{2-}$  (as discussed in Ref. 7).

From the above discussion it is clear that actually  $C_{60}$  and CP are very close in their nature to each other: both have extended  $\pi$ -electrons of low dimensionality, due to which ST effects are pronounced and ST states with their local electronic levels in the gap are important. Both CP and  $C_{60}$  can be doped e.g. by K or Na, increasing conductivity, by formation of semiconducting and metallic states. So it is not surprising that their composites and junctions, show interesting properties, which are actually determined by interactions between their ST charged and neutral excitations. Therefore let below analyze what type of interactions are possible. Since the electronic levels are close in energy (within the  $2\Delta$  gap of CP), the "chemical reactions type" interactions should be important, resulting in rechargings and transformations of ST excitations.

### 4.3 $C_{60}$ -Conducting Polymer D-A Photocell

Let us now turn to  $C_{60}$ /CP heterojunctions, which actually resembles the model of molecular type Donor-Acceptor diode of Aviram and Ratner<sup>27</sup>. In the  $Al/C_{60}/CP/Au$  layer structure, photoresponse was observed upon light irradiation as shown in Fig.8 (a). In this case, it should be noted (in this figure OO-PPV which was used as a CP) large polarity effect was also observed. The sample was irradiated by monochromated light from the side of semitransparent Au electrode deposited on glass.

In the case of forward bias (that is, Au electrode is positively biased) larger dark current has been observed than in the backward bias (Au is negative) in consistency with D-A rectification<sup>27</sup>, since OO-PPV is a donor and  $C_{60}$  is an acceptor in this D-A rectifier, as sketched at Fig.9. The original idea of Aviram and Ratner was to inject electrons to LUMO of A-molecule at forward bias from low work function electrode (Al in our case), and to inject holes to HOMO of D from hole injecting contact (Au in our case), so that recombination of  $e^-$  and  $h^+$  at interface will complete the forward dark current as sketched at Fig.9. Clearly at backward bias such process needs much higher voltage for the transmission of current, providing rectification as observed in our case, with the only difference that charges are not free  $e^-$  and  $h^+$  on molecular levels, but rather  $P^+$  and  $P_c^-$  on the corresponding local levels of polarons.

Same D-A layer upon light irradiation provides photoinduced charge separation at the interface due to favorable transfer of  $e^-$  from HOMO of D (or Ex-P level of OO-PPV in our case) to LUMO of A (to  $t_{1g}$  or  $t_{1u}$  levels of  $C_{60}$ ) or hole transfer from  $h_u$  level of  $C_{60}$  to valence band of polymer, followed by self trapping to corresponding polaronic states, providing photovoltage at open circuit or photocurrent (if short circuited or upon backward bias).

Upon photoexcitation indeed at the backward bias large signal was observed in the range of photon energy near the band gap. In the spectrum, photoresponse was also found at around 680 nm which corresponds to the transition from  $h_u \rightarrow t_{1u}$  in  $C_{60}$ . However, much smaller signal was observed at the wavelength larger than the band gap of OO-PPV and the

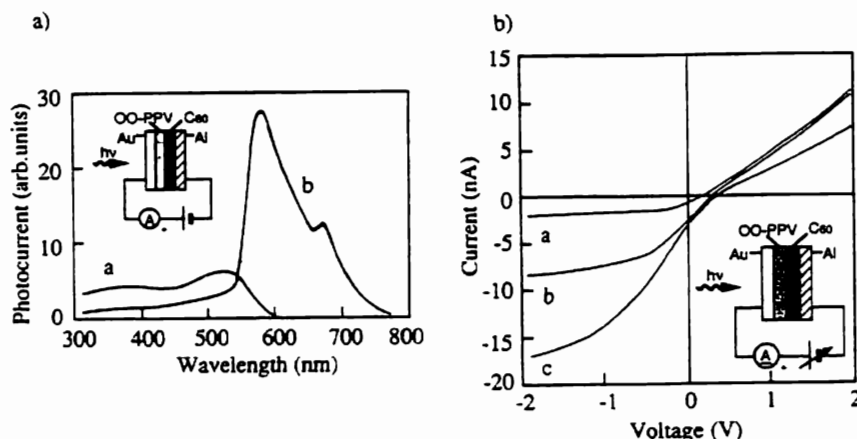


Fig.8 a) Wavelength dependence of photocurrent in  $Al/C_{60}/OO-PPV/Au$  structure: a-1(V) b-1(V), b) Current-voltage characteristics of  $Al/C_{60}/OO-PPV/Au$  structure under photoirradiation of various wavelengths. a360nm b550nm c560nm

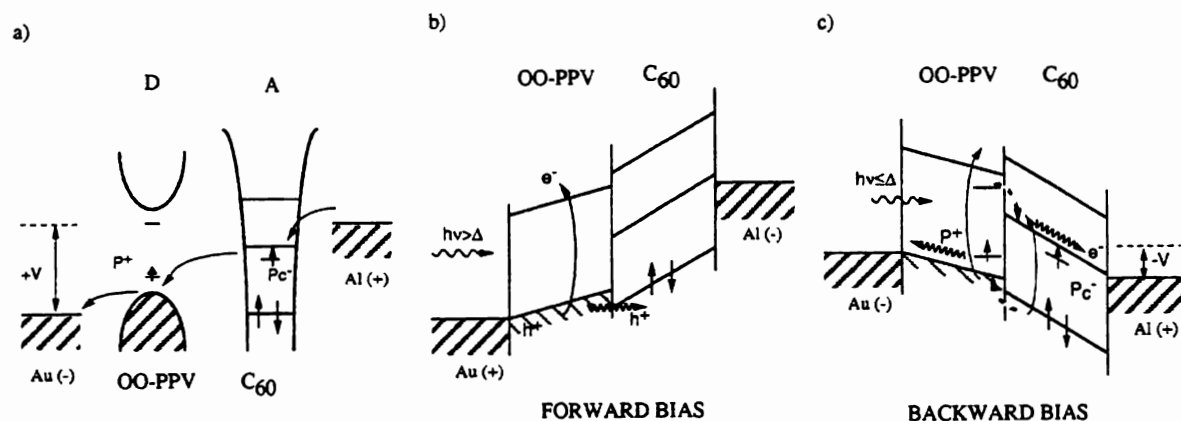


Fig.9 a) Rectification in D-A molecular layer diode at forward bias  $V > 0$ , under dark conditions, b) photogeneration of e-h pairs at the electrode region; photoinduced charge transfer at interface is not important, c) photoinduced charge transfer at  $C_{60}$ /OO-PPV interface (shown by solid arrows) contributes to enhanced photoresponse at  $h\nu < \Delta$ .

response at higher photon energy was negligible.

On the other hand in the case of positive polarity (Au is positively biased) photoresponse was only observed at photon energy larger than the band gap energy as shown at Fig.8. The corresponding open circuit voltage  $V_{oc} = 0.2$  V at 560-580 nm excitation, while the short circuit current  $I_{sc} = 3$  nA is comparatively small due to large resistance of the thick enough layer of insulating  $C_{60}$ .

It should be also noted in Fig.8b that the current-voltage characteristics of this layered structure element was strongly dependent on the wavelength of the excitation. That is, for the photon energy much larger than the band gap energy of OO-PPV, the photoresponse for the backward bias saturates with increasing voltage. On the other hand, that at photon energies around the band gap photocurrent increased more with voltage.

These results on  $Al/C_{60}/OO-PPV/Au$  layers can be explained as follows. In the case of backward bias, the response should be due to the PCT between OO-PPV and  $C_{60}$  crossing the junction as sketched at Fig.8c. Photo-separated  $P^+$  in OO-PPV and  $P_c^-$  in  $C_{60}$  layers drift down the potential and are collected at electrodes. Note that electric field drop is mainly in  $C_{60}$  layer due to its higher resistance. This behavior is quite similar to the photocurrent enhancement in the conventional p-n type photodiode at backward bias. However the light with energy much larger than the band gap of OO-PPV does not reach the junction area due to large absorption in the bulk of OO-PPV. Therefore the response is mainly observed in the region around the band gap energy, where Ex-P excited at the interface can dissociate into  $P^+$  and  $P_c^-$  due to  $e^-$  transfer. At 680 nm the  $h\nu \rightarrow t_{1u}$  transition in  $C_{60}$  layer is also possible followed by  $h^+$  transfer to OO-PPV layer (Fig.9c), which gives a small peak in photoresponse at backward bias of Fig.8a.

On the other hand, in the case of positive bias the carriers excited near the Au electrode by light of photon energy larger than the band gap can contribute to the photoresponse, since  $P^+$  from OO-PPV will be drifted to Au, while  $P^+$  may drift up the electric field and can be collected at Al electrode if there exists chance to cross the interface due to thermal excitation or tunneling across the barrier between OO-PPV and  $C_{60}$ , shown at Fig.9b. In this case also the light with the energy around the band gap can reach the junction area and create photo-separated carriers. However, because the polarity of Al is positive, the electron even if have been transferred to  $C_{60}$ , can not be collected at Au electrode (and hole in  $P^+$  separated at interface can not be collected at Au electrode), and thus not contributing to photocurrent, resulting thus in the negligible response for positive bias.

The saturation in current-voltage characteristics observed for backward bias can be interpreted as follows. The excited

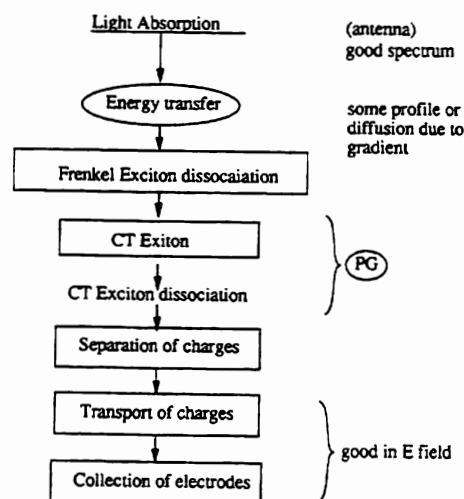


Fig.10 The scenario of the photoresponse in D-A type photocell.

carrier density at around junction by light with photon energy much larger than the band gap is very low because such light is attenuated strongly by the absorption of OO-PPV. In such a case, the saturation effect can occur as observed in the experiment due to the limited concentration of excitons (or P in OO-PPV) to provide the electron for the transfer from OO-PPV to  $C_{60}$ . That is, in this case the photoexcitations generation is rate determining factor for the photoresponse. Therefore, with increasing light intensity, the number of carriers separated across the interface also increases and the saturation field in the current-voltage characteristics, needed to collect all this carriers should shift to higher voltage.

So the effect of PCT between OO-PPV and  $C_{60}$  takes place only at the interface region, due to dissociation of neutral photoexcitations both in  $C_{60}$  and OO-PPV, which can be influenced by electric field. This PCT contributes to photocurrent only upon backward bias (and give sizable photovoltaic effect with  $V_{oc}=0.2V$ ), while the carriers generated at the electrode regions give rise of photocurrent at forward bias.

The general scenario of photophysical processes in double layer D-A photocell is shown at Fig.10.

The main processes, which take place and determine the efficiency of photon energy conversion are following:

1. Absorption of photons.
2. Diffusion of excitons towards D-A interface.
3. Collection of excitons and their dissociation at the interface.
4. CT at interface and back recombinative CT.
5. Diffusion (or slow drift in electric field) of charge carriers towards ohmic electrodes and their collection. This processes depend on the energetics of D-A heterojunction, spectral range of pumping photons and geometry as qualitatively sketched at Fig.11.

To improve the performance of photocells we discuss below the several possibilities in multilayered structures in which the number of useful interfaces effective for PCT is increased.

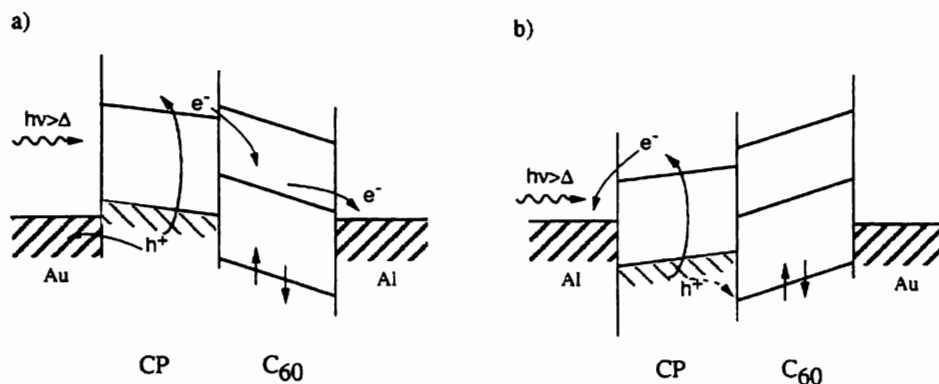


Fig.11 Effect of attached electrodes to D-A structure. a) Au/CP/ $C_{60}$ /Al : This type should have better quantum efficiency, because there is no barrier to  $e^-$  and  $h^+$  and they can easily reach to external circuit. b) Al/CP/ $C_{60}$ /Au : This type should have worse quantum efficiency, because most of  $h^+$  will be blocked at CP- $C_{60}$  interface.

## 5. PROSPECTS TO INCREASE EFFICIENCY OF PHOTOCELLS IN MULTILAYERED STRUCTURES

Organic multilayered structures (OMS) have become recently attractive subject for experimental and theoretical studies<sup>28-33</sup>. The progress with the molecular beam epitaxial growth of ultrathin layers allowed to fabricate OMS of the same good quality as inorganic quantum well structures (QWS)<sup>28-31</sup>. A number of interesting phenomena have been already found in their optical and photophysical properties, including the observation of the blue shift of photoluminescence with decrease of the OMS period<sup>29,30</sup>, the spectral changes in electroluminescence<sup>30,31</sup> and electric field modulation of photoluminescence upon applied backward bias voltage<sup>31</sup>.

These results are usually interpreted in terms of size quantization and large radius excitons, similar to ideas of quantum well structures of inorganic semiconductors.

Agranovich has pointed out recently that molecular excitons may have many interesting novel properties at the interfaces of OMS<sup>32,33</sup>, and was able to explain the observed blue shift of luminescence in OMS<sup>29-31</sup> in terms of Frenkel excitons<sup>32</sup>.

Below we show that behavior of charge carriers at the interfaces in OMS and molecular heterojunctions also can be quite different from that in p/n junctions, and demonstrate how photogeneration can be increased in  $C_{60}$ -CP OMS photocells due to formation of appropriate type of polarization double barriers<sup>4</sup> (PDB).

## 5.1. Polarization Double Barrier formation in OMS

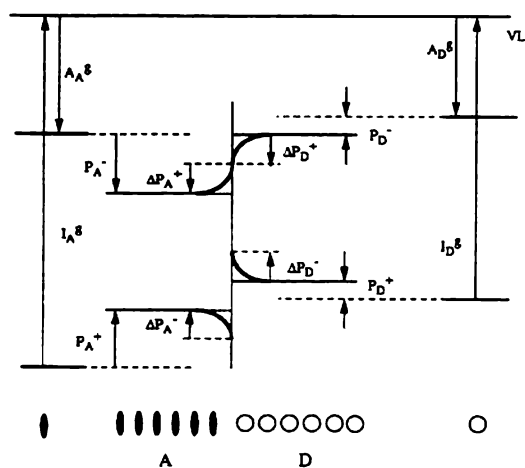


Fig.12 PDB formation in D-A heterostructure.

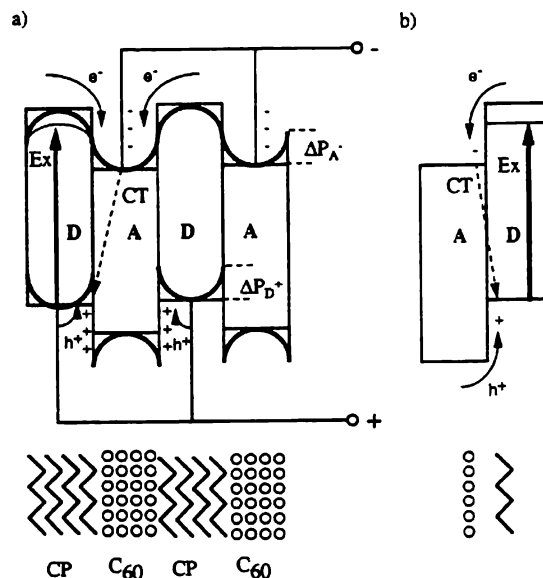


Fig.13 Schematic diagram of type 1' QWS photocell with PDB. a) Multilayered structure. b) single heterostructure.

Here we show that behavior of charge carriers at the interfaces in OMS and molecular heterojunctions also can be quite different from those of inorganic quantum wells and p-n junctions due to their localized character and features of the polarization energy at the boundaries between molecular layers.

We have discussed recently in details the physics of PDB formation<sup>12</sup> and here we will discuss its effect on photogeneration and on the anisotropic photoconductivity of multilayered structures, and particularly on the photovoltaic response of C<sub>60</sub>-CP type multilayered structures.

Let start with demonstration on the qualitative level how PDB appears on the simple model of the interface between N layers of D and A, as shown at Fig.12. If the D molecule in the bulk of D layer is ionized then its ionization potential  $I_D$  and electron affinity  $A_D$  should be shifted by polarization energies of hole  $P_D^+$  and of electron  $P_D^-$  respectively to their gas phase values:

$$I_D = I_D^s - P_D^+, A_D = A_D^s + P_D^-.$$

It means actually that the HOMO-LUMO separation in the solid state of D, i.e. the gap energy for e-h pair creation, should be much smaller then that in the gas phase (used earlier in Fig.12. Similarly the  $P_A^+$  and  $P_A^-$  should shift levels of A, as shown at Fig.13. a)

The important point is that  $P$  can be varied in wide range from 1 to 3.5 eV in different molecular solids, as found in photoemission studies depending on their molecular polarizability  $a$  and intermolecular separation  $d(n-m)$ , since in a simple approximation  $P$  is determined as

$$P_{nm} = d_m E_{nm} = -ae^2/2 = -ae^2/2(n-m)^4$$

Let assume that  $P_D \ll P_A$ , which can be achieved practically taking rubrene molecules as D and p-iodanil as A.

The key idea, which we stress here is that for the molecules at the interface  $P$  should be different from the bulk value, since the charge interacts not only with the host molecules, but also with the molecules on the other side of interface, which have different  $a$  and  $d$ , and hence  $P$ . It is clear then that  $P_D(1)^+$  and  $P_D(1)^-$  of the first layer at the interface should be larger than in the bulk, since charges at the interface interact with largely polarizable molecules of A, while  $P_A(1)^+$  and  $P_A(1)^-$  at the first layer of A should be smaller than bulk values due to opposite effect of interaction with less polarizable molecules. The corresponding values at next layers  $P(2)$ ,  $P(3)$ , .. should change converging to bulk values, actual values of  $P(n)$  being estimated in, giving for a chosen rubrene-p-iodanil pair the  $\Delta P = P - P(1) = 0.2 - 0.4$  eV, both for e and h.

This changes of  $P$  mean that the band gap in D is decreased by  $\Delta P_D^+ + \Delta P_D^-$ , while the band gap of A is increased by  $\Delta P_A^+ + \Delta P_A^-$  at the interface compared to their bulk values, leading thus to formation of PDB potential relief at the interface. Depending on properties of single molecules in each molecular layer, PDB can lead to selective charge injection from one layer to another or charge confinement at the interfaces and may influence significantly photophysical and optical proper-

ties of organic superlattices.

## 5.2 Unimolecular D-A Photocell

To demonstrate how the solid state effect of PDB may influence the D-M-A let us recall first processes in D-A unimolecular rectifier<sup>27</sup> shown at Fig.14. This D-A pair may provide the photoinduced charges separation, upon excitation of D or A molecules in their absorption bands, since energetically favorable transition of photoexcited electron from LUMO of D to LUMO of A (or hole injection from HOMO of A to that of D) will give photocurrent (or photovoltage). Actually this type of photoinduced charge transfer takes place in e.g. C<sub>60</sub>-conjugated polymer photocells where C<sub>60</sub> plays role of A, while D is a polymeric chain. That is photovoltaic effects observed in C<sub>60</sub>/CP<sup>10,13,22</sup> can be interpreted in terms of this D-A model.<sup>22</sup> Since the process is limited by quick back recombination CT, one can try to avoid back CT by placing a secondary A<sub>2</sub> next to A (or secondary D<sub>2</sub> next to D), so that charges should be further spatially separated to A<sub>2</sub> (or D<sub>2</sub>), suppressing quick back CT, similar to the processes in natural photosynthetic units of plants or bacteria. Actually this strategy has been used to achieve a sizable photocurrent in LB film molecular photocells<sup>9</sup>. Note however that here the secondary A<sub>2</sub> and D<sub>2</sub> are molecules chemically different from primary A and D. The third A<sub>3</sub> and D<sub>3</sub> are also different.

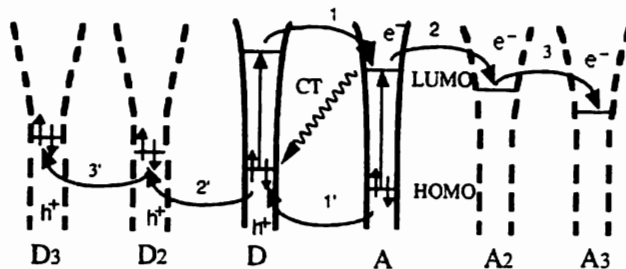


Fig.14 Schematic energy diagram of unimolecular rectifier. D<sub>2</sub> and A<sub>2</sub> should suppress the back CT from A to D.

## 5.3. Photogeneration in OMS

Type I' superlattice. Now for the type I' QWS shown at Fig. 12 which requires

$$A_D^s + P_D > A_A^s + P_A, \text{ but } I_D^s - P_D > I_A^s - P_A$$

one have two main types of PDB structures depending on relations between  $P_D$  and  $P_A$ :

- if  $P_D < P_A$ , we have a "half collecting PDB" since only electrons should be collected to the center of B, while holes can be captured at the interface regions of A. This is the case of C<sub>60</sub>-CP.
- if  $P_D > P_A$  one has a "half confining PDB" since holes can be separated selectively into A parts depending on the relative offset of valence bands.

Let now demonstrate how photogeneration (PG) can be increased on the example of C<sub>60</sub>-CP, OMS sketched at Fig.13. Without PDB (i.e. for a pair of DA layers, for which solid state effect of P is absent, or for D and A solids with similar P) there are no bendings of electronic levels and upon photoexcitation of CP layer, the exciton (Ex) can dissociate by e<sup>-</sup> transfer to C<sub>60</sub> while hole is blocked in CP (see Fig.13a). The disadvantages of this photogeneration process are obvious:

- Only one layer from each side is involved into the process, i.e. PCT occurs only at the narrow bilayer interface.
- The back CT will quickly lead to recombination, since charges are very close to each other on adjacent layers.

At account of PDB the bending of levels should appear on each side of interface, which corresponds to attraction of Ex and both charges e<sup>-</sup> and h<sup>+</sup> in CP to C<sub>60</sub> layers but to repulsion of Ex and e<sup>-</sup>, h<sup>+</sup> existing in C<sub>60</sub> side from the CP. We assumed here that C<sub>60</sub> has much higher polarizability and thus higher  $P_A$ . Now due to PDB existence from 3 to 4 layers on each side will participate in PG process:

- Excitons photogenerated in CP will favorably diffuse down the PDB towards interface and when encountering the last CP layer, should dissociate due to e<sup>-</sup> transfer into the first layer of C<sub>60</sub> film, where it will be self-trapped into ring type polaron  $P_c^-$ :  $Ex + C_{60} = P^+ + P_c^-$ . Remaining polaron in the CP chain ( $P^+$ ) should be confined in the well of PDB in CP.
- Due to PDB profile in C<sub>60</sub> layer this  $P_c^-$  will be repulsed from the interface further into the volume of C<sub>60</sub>, i.e. it will be pulled inside the C<sub>60</sub> film, due to the gain of polarization energy deep in the volume.
- Now back CT of e<sup>-</sup> from  $P_c^-$  to CP, i.e. recombination with  $P^+$  should be suppressed since  $P_c^-$  is specially separated far from  $P^+$ . Note however that  $P^+$  confined in the well in CP side should create a space charge layer, which will influence the equilibrium concentration of photogenerated carriers.

The photoconductivity of such OMS in the direction parallel to the interface should be significantly increased since both e<sup>-</sup> and h<sup>+</sup> spatially separated ( and captured in the different parts of each layer ) can contribute to current.

Contrary PC in perpendicular direction should be much smaller, so remarkably anisotropic PC is expected (see also discussion in Ref.33).

- 4) If appropriate ohmic contacts are attached to A and D layers as sketched at Fig.13a), then enhanced photovoltaic effect is expected, since the net area of interface which is effective in photogeneration (PG) is increased  $N$  times, where  $N$  is the number of DA layers in the superlattice. So summarizing we point that PDB allows to increase the effective width of the interface region which contributes to PG, while arrangement into organic superlattice will increase the net interface area, both effects increasing thus the efficiency of PG and the performance of OMS photocells.

Below we show how matching the energy levels of D,M and A and selecting a proper type of PDB the appropriate potential profile can be formed at the interface which will help to separate carriers of one sign, and moreover, suppress their back charge transfer relaxation.

#### 5.4 Multilayered D-M-A photocell, with photon pump layer

Let now analyze the behavior of photogenerated carriers in D-M-A cell of Fig.15. Assume that photons are absorbed mainly in M-layer (which is chosen as a good light absorber) creating Frenkel excitons, which should move to the interface region due to similar polarization forces (as those creating PDB) as recently shown by Agranovich<sup>24</sup> and dissociates into free  $e^-h^+$  pairs (details of influence of PDB on photogeneration process are discussed in Refs.12,21). Due to PDB both  $e^-$  and  $h^+$  should drift in the potential well towards the interface and  $e^-$  will meet the accelerating potential from the layer A side (due to lower LUMO in A) while  $h^+$  will meet a barrier due to lower HOMO in A, and oppositely in the D side PDB:  $h^+$  accelerated, and  $e^-$  blocked.

So  $e^-$  should be pulled into A hopping down to LUMOs of each next layer of A, which are acting as secondary acceptors, similar to that of Fig.14. In our case however chemically identical A molecules provide this property of favorable charge transfer further from the interface into the bulk of layer A.

Thus the net effect of first PDB at the AM interface is the selective separation of only  $e^-$ , photogenerated in M across the interface into layer A (where they can be collected at ohmic contact), while holes separated selectively by second PDB at M-D interface into layer D should be collected at its ohmic contact. Note however that if both charges are photogenerated in layers A and D they can not be easily separated into M, because both are repulsed from the interface by PDB back into the volume. So layers A and D acts only as collector of charges while M as absorber which injects carriers, so it plays role of "photon pump" layer as in photosynthetic units. However note that charging of the interface regions by oppositely signed carriers confined in well parts of PDB during the operation of the photocell, may decrease the photoseparation, and thus limit the photocurrent (photovoltage) depending on the photoexcitation intensity and relative values of PDB parts on both sides of interfaces.

By repeating AMD units the organic superlattice photocell can be arranged in which the interface area should be dramatically increased<sup>12,21</sup>, while the semitransparent ohmic contacts to A and D can be spatially separated (as sketched below) further increasing the performance of photocell.

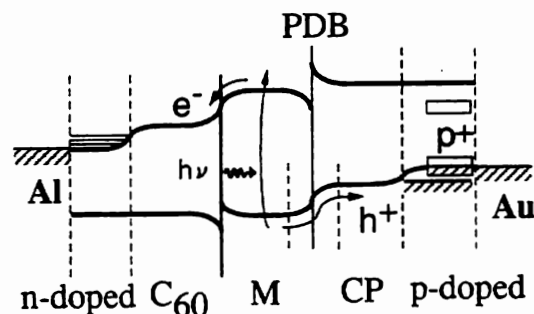


Fig.15 Schematic energy diagram of D-M-A type photocell. M: photon pump layer.



#### 6. SUPERCONDUCTIVITY IN DOUBLY DOPED (by $C_{60}$ and K) CONDUCTING POLYMERS

In all above studies carriers appeared in  $CP(C_{60})_y$  composites only upon photoexcitation, while in dark conditions the conductivity of the composite was very low.

However it is interesting to study the effects of strong ground state CT by n- or p-type doping of such composites, when charge carriers can be transferred from a second intercalant (K or  $I_2$ ) filling the bands of CP and empty LUMO levels of  $C_{60}$  molecules. Such strong doping should actually create a novel type of  $\pi$ -electron system in which charged  $C_{60}^{\pm}$  anions

should be coexisting (in ideal) with the sea of mobile charges on CP chains  $\pi$ -electron network. Optical and conductive properties of such system are very intriguing, while at low temperatures SC phases can be expected.

Naturally if  $C_{60}$  in a composite is aggregated into clusters<sup>14,15</sup> in the case of high  $C_{60}$  content  $y > 5$  mol %, then  $K_3C_{60}$  granules, connected by proximity effect through conducting CP, or by Josephson junctions through insulating CP barriers, may give disordered granular SC.

However more exciting is the possibility to realize truly microscopic molecular level of superconducting phase, in which SC pairing of electrons in CP chains may be induced (or enhanced) via the hybridization to molecular  $C_{60}^{n-}$  subsystem. It is recognized that  $C_{60}$  molecules have an effective electron-electron attraction, as suggested by intramolecular origin of SC pairing (either of vibronic or of electronic origins) in fulleride superconductors.

Recently we have studied such strong doping effect in  $CP(C_{60})_y$  composite by alkali metals, and have found the superconducting (SC) phase<sup>14,15</sup> using LFMA/ESR combined method and SQUID magnetometer. We also have revealed unusual magnetic properties of this superconducting composites. Below we give a brief summary of SC results in K doped  $CP(C_{60})_y$  and outline the future problems here.

The K-doping is performed step by step at rather low temperatures  $T_d = 120/110$  °C ( $T(\text{film})/T(K)$ ) compared to typical  $T_d$  for vapor K-doping of fullerides to avoid melting of PAT matrix, and each step is monitored by ESR spectrometer. to analyze the appearance and evolution of spins (and hence charge carriers) both on PAT and  $C_{60}$  components of the composite. Existence of SC phase in each step is checked by the LFMA using same spectrometer.

The measurement of nonresonant microwave absorption in low magnetic field (so called LFMA or LFS) in fullerides has been proved to be a unique method for the search of SC phases. To make sure that LFMA is not misinterpreted, we additionally prove the existence of SC phase by SQUID magnetometry.

Figure 16 shows characteristic LFMA spectra of composite of  $y=0.5$  mol % at various temperatures below  $T_c$ . Contrary to LFMA of bulk  $K_3C_{60}$ , that of  $PAT(C_{60})_yK_x$  composite showed rather narrow hysteresis and the phase of LFMA sometimes changed to opposite at a temperature close to  $T_c$ , which depends on K-doping level  $x$ . Figure 17 shows temperature dependence of LFMA peak to peak intensity  $dP/dH$  for  $y=0.5$  and  $y=5$  mol %. LFMA abruptly disappeared at  $T_c$ , which is typical to LFMA of superconducting origin. The  $T_c$  found as LFMA onset, and intensity of LFMA, both increased with increase of doping time, and attained up to 17.5 K in the best sample of optimally doped composites with  $y=5$  mol %.

It should be mentioned that  $T_c$  of the composite film is still low compared to that ( $T_c=19K$ ) of bulky  $K_3C_{60}$ , while the LFMA intensity of the composite is higher than that of bulky  $K_3C_{60}$ . This intensive LFMA seems to come not from the bulk

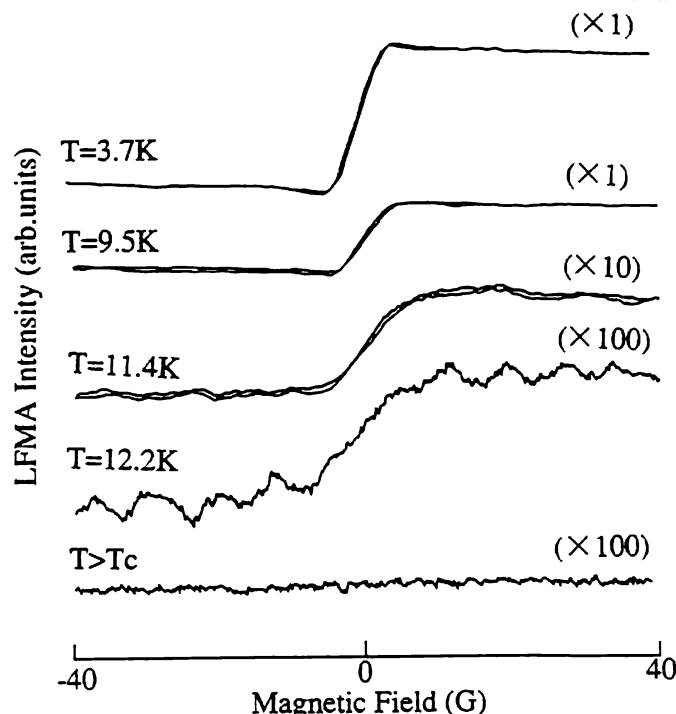


Fig.16 LFMA of superconducting  $PAT(C_{60})_{0.005}K_x$  composite, with small  $C_{60}$  content (0.5 mol %) at different  $T$  below  $T_c$ .

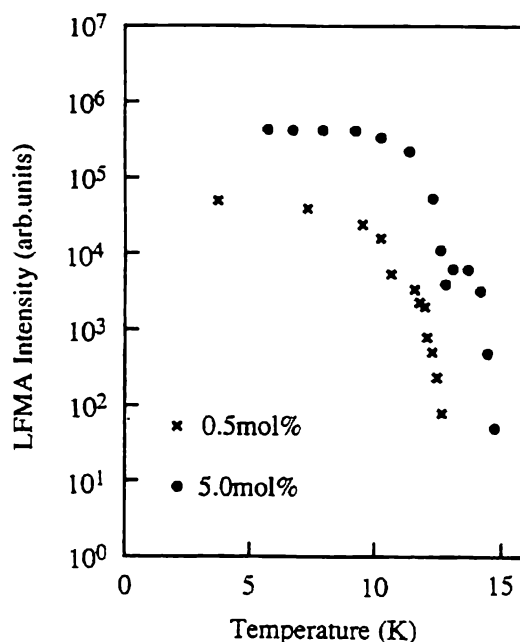


Fig.17 Temperature dependence of LFMA peak to peak intensity in  $PAT(C_{60})_yK_x$  composite of  $y=0.5\text{mol}\%$  and  $y=5\text{mol}\%$ .

SC, but from the intergrain weak links which are known to contribute largely to LFMA intensity through low viscosity of fluxons in Josephson junctions. The hysteresis loop of LFMA increases with the decrease of modulation amplitude, in a typical way for SC grains weakly coupled network. Rather low  $T_c$  compared to that of bulk  $K_3C_{60}$  SC phase suggests the important role of imperfections and interface effects, which are natural for disordered  $K_3C_{60}$  small grains. Mesoscopic effects in Josephson network usually result in effective  $T_c$  lower than bulky  $T_c$ . The change of derivative LFMA phase at a temperature close to  $T_c$  is indicative of the anomalous zero-field maximum in direct absorption, which is connected with the granular nature of SC in a percolative media. However if negative phase of LFMA survives till low temperature  $T \ll T_c$ , this might be indication of the existence of so called Josephson p-junctions, containing unpaired spin in the barrier. We have found such behavior in our high  $y$  samples and discuss in detail its correlations with paramagnetic behavior of field cooled magnetization found in SQUID in forthcoming paper.

From the above consideration the strategy to realize truly polymeric, two-band superconductivity, induced by  $C_{60}$  molecules can be obtained.

Summarizing PAT- $C_{60}$  composites give a new type of disordered granular SC. Changing the conducting polymer host one can also monitor the conductive properties of the matrix and we are now studying SC phases in OO-PPV ( $C_{60}$ )<sub>y</sub>-K<sub>x</sub> composites.

It should be mentioned that the advantage of the conducting-polymer-fullerene system is the possibility to influence dramatically both the host polymer (making it metallic) and also the molecular  $C_{60}$  dopants with the same n-type dopant, tuning the electronic properties of clusters from insulating to superconducting. Organic S-N-S (superconductor-normal metal-superconductor) thin film structures can be created just by alkali metal doping into multilayered thin film heterojunctions of  $C_{60}$ -CP- $C_{60}$  type.

To clarify the nature and process of n-type doping into  $C_{60}$  doped CP, *in-situ* optical studies by electrochemical n-type doping utilizing thin  $C_{60}$  doped CP on ITO electrode immersed in electrolyte solution are now under progress.

### SUMMARY

Thus, we have shown that fullerenes are rather interesting and effective charge supporting agents for CP due to their 2-D  $\pi$ -electrons, high symmetry and large size, which pronounce ST.

$C_{60}$  can quickly capture electrons from levels of Ex, P/BP or S in CP chains, storing them in ring type Pc and BPc. The later is long living due to geometrically suppressed back CT. Multicharging of  $C_{60}$  by injected electrons is suggested due to suppressed Coulomb correlations on fullerene spheres.

We suggest that the efficiency of D-M-A molecular layered photocells may be enhanced in the presence of favorable PDB at interfaces with "photon pump" layers, due to the following reasons:

1. The photogeneration of charged carriers is expected to be enhanced, due to vectorial diffusion and better dissociation of Frenkel excitons in layer M towards PDB regions.
2. Separation of charges should be enhanced by PDB potential which accelerates charges of one sign deep into the collecting layer, separating them from the oppositely signed charge, (which is confined at the interface), and thus suppresses the recombination back charge transfer.

$C_{60}$  doped conducting polymer film give a new type of disordered granular superconductivity upon K doping. In-situ optical properties of  $C_{60}$  doped conducting polymer film upon n-type doping are now under study.

### ACKNOWLEDGMENTS

We thank the financial support of the ISF grant RU9000. Part of this work was supported by a Grant-in-Aid for Scientific Research on Priority Areas (No.04205097) from the Ministry of Education, Science and Culture. We would like to thank stimulating discussion with Prof. V.M.Agranovich on the nature of photogeneration at interfaces. A.A.Z. is grateful for Osaka University for hospitality.

### REFERENCES

1. S. Morita, A.A. Zakhidov and K. Yoshino, Solid State Commun., 82, 249, 1992.
2. S. Morita, A.A. Zakhidov, T. Kawai, H. Araki and K. Yoshino, Jpn. J. Appl. Phys., 31, L890, 1992.
3. K. Yoshino, X.H. Yin, S. Morita, T. Kawai and A.A. Zakhidov, Chem. Express, 7, 817, 1992, also in Solid State Commun., 85, 85, 1993.
4. K. Yoshino, X.H. Yin, A.A. Zakhidov, T. Noguchi and T. Ohnishi, Jpn. J. Appl. Phys., 32, L357, 1993.
5. S. Morita, S. Kiyomatsu, M. Fukuda, A.A. Zakhidov, K. Yoshino, K. Kikuchi and Y. Achiba, Jpn. J. Appl. Phys., 32, L1173, 1993.
6. K. Yoshino, T. Akashi, K. Yoshimoto, S. Morita, R. Sugimoto and A. Zakhidov, Solid State Commun., 90, 41, 1994.



7. K.Yoshino, X.H.Yin, T.Akashi, K.Yoshimoto, S.Morita and A.A.Zakhidov, *Mol.Cryst.Liq.Cryst.* 225, 197, 1994.
8. A.A.Zakhidov, *Proc. Int. Conf. ELORMA-87, Moscow*, pp.256, 1987 also in *Synth.Met.*, 41-43, 3393, 1991.
9. Fujihira et. al., *Thin Solid Films*, 133, 77, 1985.
- 10.N.S.Sariciftci, D.Braun, C.Zhang, V.Srdanov, A.J.Heeger, F. Wudl, *Science* 258, 1474, 1992. and also *Appl.Phys.Lett.*, 62, 585, 1993.
11. L.Smilovitz, N.S.Sariciftci, R.Wu, C.Gettinger,A.J.Heeger and F.Wudl, *Phys.Rev.B*, 47, 13835, 1993.
12. A.A.Zakhidov and K.Yoshino, *Synth.Met.*, 64/2-3, 155, 1994.
13. S.Morita, A.A.Zakhidov, K.Yoshino, *Jpn.J.Appl.Phys.*32, L873, 1993.
14. H.Araki, A.A.Zakhidov, E.Saiki, N. Yamasaki, K. Yakushi and K. Yoshino, *Jpn. J. Appl. Phys.* ( in press )
15. A.A. Zakhidov, H. Araki, K.Tada, K. Yakushi and K. Yoshino, *Phys. Lett. A* (to be published)
16. R. Sugimoto, S. Takeda, H.B. Gu and K. Yoshino, *Chem. Express*, 1, 635, 1986.
17. I. Murase, T. Ohnishi, T. Noguchi and M. Hirooka, *Polym. Commun.*, 28, 229, 1987.
18. M. Fukuda, K. Sawada and K. Yoshino, *Jpn. J. Appl. Phys.*, 28, L1433, 1989.
19. T.Masuda, T. Hamano, K. Tsuchihara and T. Higashimura, *Macromol.*, 23, 1374, 1990.
20. H.Araki, N.Yamasaki, A.A. Zakhidov and K.Yoshino, *Physica C* 233, 242, 1994.
21. K.Seki, *Mol.Cryst.Liq.Cryst.*, 171, 255, 1989.
22. S.Morita, S.B.Lee, A.A.Zakhidov and K.Yoshino, *Mol.Cryst.Liq.Cryst.*, 256, 839, 1994.
23. Y.Wang, R.West and Chien-Hua Yuan, *J.Am.Chem.Soc.*, 115, 3844, 1993.
24. A.A.Zakhidov, K.Tada and K.Yoshino, *Synth.Metals* 71, 2113, 1995.
25. K.Yoshino, T.Akashi, K.Yoshimoto, S.Morita, T.Kawai and A.A.Zakhidov, *Jpn.J.Appl.Phys.*, 34, L127, 1995.
26. K.Yoshino, K.Yoshimoto, M.Hamaguchi, T.Kawai, A.A.Zakhidov, H.Ueno, M.Kakimoto and H.Kojima, *Jpn.J.Appl.Phys.*, 34, L141, 1995.
27. A.Aviram and M.A.Ratnar, *Chem. Phys. Lett.*, 29, 277, 1995.
28. F.F.So, S.B.Forest, Y.Q.Shi and W.H.Steier, *Appl.Phys.Lett.*,56, 674, 1990.
29. F.F.So and S.B.Forest, *Phys.Rev.Lett.*, 66, 2649, 1991.
30. Y.Ohmori,A.Fujii, M.Uchida,C.Morishima and K.Yoshino, *Appl. Phys. Lett.*,62, 3250, 1991.
31. Y.Ohmori,A.Fujii, M.Uchida,C.Morishima and K.Yoshino, *Appl. Phys. Lett.*,63, 1871, 1993.
32. V.M.Agranovich, *Mol.Cryst.Liq.Cryst*, 228, 3, 1993.
33. V.M.Agranovich, *Physica Scripta*.(in press )
34. V.M.Agranovich, *Mol.Cryst.Liq.Cryst*, 230, 3, 1993.